7-2022

Characterization of Pyrrolidinyl-hexahydro-pyranopiperazines as a Novel Kappa Opioid Receptor Agonist Scaffold

Brian Reed

Michael Miller

Mayako Michino

Eduardo R. Butelman

Ariel Ben-Ezra

See next page for additional authors

Authors

Brian Reed, Michael Miller, Mayako Michino, Eduardo R. Butelman, Ariel Ben-Ezra, Philip Pikus, Michelle Morochnik, Yuli Kim, Amy Ripka, Joseph Vacca, and Mary Jeanne Kreek

ACS Chemical Neuroscience

pubs.acs.org/chemneuro

Letter

Characterization of Pyrrolidinyl-hexahydro-pyranopiperazines as a Novel Kappa Opioid Receptor Agonist Scaffold

Brian Reed,*[,†] Michael Miller,[†] Mayako Michino, Eduardo R. Butelman, Ariel Ben-Ezra, Philip Pikus, Michelle Morochnik, Yuli Kim, Amy Ripka, Joseph Vacca, and Mary Jeanne Kreek

Cite This: *ACS Chem. Neurosci.* 2022, 13, 1849−1856

Read Online

ACCESS | Metrics & More | Article Recommendations | Supporting Information

ABSTRACT: The kappa agonist structure−activity relationship around the novel, pyrrolidinyl substituted pyranopiperazine scaffold was developed. More specifically, the dichloroPhenylAcetamide-Pyrrolidinyl-PyranoPiperazine (PAPPP) core A was the focus of our work. The modulation of kappa receptor potency/G-protein activation and arrestin recruitment with respect to changes of the piperazine R group in A was demonstrated. Reduced β_2-arrestin recruitment and differential G-protein bias were observed for select analogues. To better understand the subtlety in receptor signaling, analogues were profiled as the resolved enantiomers. To determine *in vivo* target engagement, a subset of compounds was tested in mice for stimulation of serum prolactin, a neuroendocrine biomarker of KOR-agonist effects. Additional *in vivo* characterization included measurement of potential unwanted effects of kappa receptor activation such as sedation. These studies demonstrate a novel kappa receptor agonist scaffold with potential for G-protein signaling bias to probe *in vivo* pharmacology.

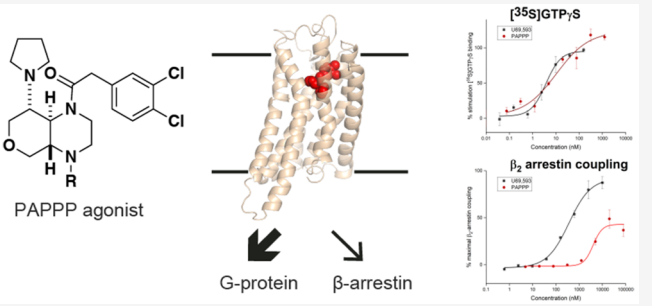

KEYWORDS: *kappa agonist, kappa receptor, opioid receptor, biased agonist*

The endogenous opioid system, consisting of the endogenous opioid peptides and the mu, kappa, and delta opioid receptors and the related NOP receptor, is involved in diverse physiological processes, including those underlying pain/analgesia and reward/euphoria, as long recognized in pharmacological characterization studies of compounds derived from opium and synthetic derivatives thereof. The first known compounds that were identified as acting on the endogenous opioid system gave the system its name, as these were compounds or derivatives of compounds containing a common morphinan backbone found in the opium plant, *Papaver somniferum*. Studies of diverse effects of morphinan containing compounds as well as select non-morphinan containing compounds such as ketocyclazocine led to the identification of the three G-protein coupled opioid receptor systems (mu, kappa, and delta opioid receptors; MOR, KOR, and DOR, respectively) and elucidation of their distinct but overlapping pharmacology.

Many compounds have been synthesized that interact with the opioid receptors, leading to the development of a rich pharmacological compendium of compounds for targeting the opioid system, improving our understanding of the structural basis for discriminative binding among the three receptors as well as activation or blockade.[1] A recent advancement in the understanding of the biochemistry of G-protein coupled receptors (GPCRs) is that intracellular signaling following agonist activation can be mediated by not only G-protein activation but also by another directly coupled scaffolding protein, β-arrestin,[2] as well as potentially other pathways. Given the diverse *in vivo* effects of opioid agonists, there is the possibility that some of the effects may predominantly arise from activity resulting from only one of these signaling pathways. Identification of biased agonists pathways would improve our understanding of the differential roles of individual signaling pathways in causing specific effects. Such compounds may yield improved therapeutics with fewer side effects.

In our efforts to develop a novel class of KOR agonists, we commenced our synthetic efforts based initially on published work from the laboratory of Wünsch.[3] They reported a novel *trans,trans*-configured perhydroquinoxaline scaffold, combining elements of the well-characterized canonical U50,488 KOR agonist with the highly potent KOR agonist GR-89,696. Derivatives of this scaffold exhibit potent KOR binding as well as partial or full KOR agonism in a [^{35}S]GTPγS assay.[3,4] We have subsequently modified this scaffold to insert an oxygen atom in the cyclohexyl fragment of the perhydroquinoxaline

Received: April 29, 2022
Accepted: June 14, 2022
Published: June 23, 2022

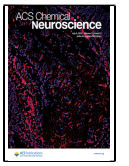

https://doi.org/10.1021/acschemneuro.2c00258
ACS Chem. Neurosci. 2022, 13, 1849−1856

ring system (Figure 1). We report here the synthesis (detailed in the Supporting Information) and *in vivo* and *in vitro*

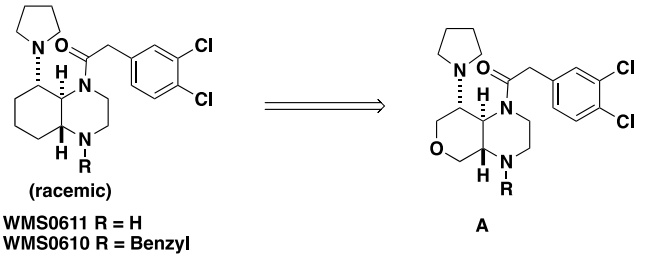

Figure 1. PAPPP scaffold.

characterization of this scaffold with particular focus on the binding and activation of KOR. All compounds were shown to be greater than 95% pure by liquid chromatography/mass spectrometry.

Racemic mixtures of the novel PhenylAcetamide-Pyrrolidine-PyranoPiperazine (PAPPP) scaffold were initially profiled to explore the general structure−activity relationship of the arylacetamide (N1) and amino (C8) substituents of the scaffold (Table 1). As described in the Methods section, compounds were assessed in binding assays with KOR-expressing cell membranes and inhibition of [^{3}H]U69,593 as well as activity assays including stimulation of [^{35}S]GTPγS binding to determine the potency and efficacy of agonism. The degree of stimulation (efficacy) is normalized to that observed with U69,593, defined as 100% [^{35}S]GTPγS binding. For all compounds, reported values reflect a minimum of three experiments conducted on different days, with four replicates of each concentration. Compound **6**, which is the matched molecular pair of the Wünsch compound WMS-0611 (3,4), showed a KOR binding affinity of 52 nM and full agonist functional efficacy of 51 nM (Emax = 92%) in the [^{35}S]GTPγS assay. We found the 3,4-dichloro substitution on the phenyl

Table 1. KOR Binding and Functional Agonist Data (Racemic)

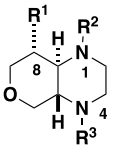

Example	R^1	R^2	R^3	KOR binding K_i, nM	KOR GTPgS EC50, nM (% act)
U69,593				7.07 ± 0.98	8.8 ± 15 (100±4%)
WMS0611				34 ± 9	240 ± 86 (68±5%)
WMS0610				260 ± 10	140 ± 10 (87±18%)
1		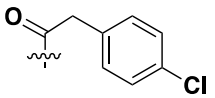	H	340 ± 30	ND
2		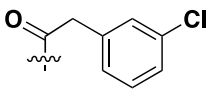	H	430 ± 100	ND
3		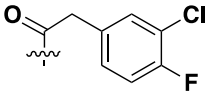	H	180 ± 20	390 ± 100 (93±8%)
4		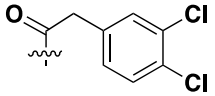	H	110 ± 10	350 ± 22 (71±7%)
5	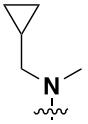	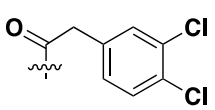	H	210 ± 30	290 ± 99 (79±3%)
6	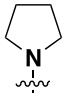	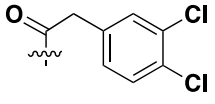	H	52 ± 17	51 ± 5.0 (92±17%)
7	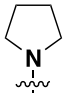	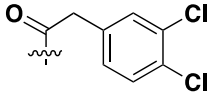	Me	36 ± 8	52 ± 2.0 (83±18%)

https://doi.org/10.1021/acschemneuro.2c00258
ACS Chem. Neurosci. 2022, 13, 1849−1856

Table 2. KOR Binding and Functional Agonist Data (Single Enantiomer)

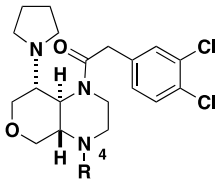

Example	R	KOR binding K_i, nM	KOR GTPgS EC50, nM (% act)	β-arrestin EC50 nM(% stim)	G-protein	
					Bias factor	95% CI
6a	H	45 ± 16	25 ± 2.8 (96±10%)	11000 ± 4000 (67±6%)	1.00	0.30
6b		50 ± 11	46 ± 5.4 (98±4%)	10000 ± 4000 (53±12%)	0.84	0.51
7a	Me	24 ± 6	83 ± 3.3 (92±23%)	20000 ± 5500 (52±4%)	0.85	0.26
7b		48 ± 22	31 ± 17 (86±12%)	22000 ± 750 (53±16%)	1.27	0.50
8a		4.8 ± 0.5	3.8 ± 0.6 (135±16%)	3100 ± 1300 (100±2%)	1.27	0.20
8b		16 ± 3	4.3 ± 0.5 (93±12%)	3800 ± 1500 (99±8%)	1.14	0.21
9a		3.1 ± 0.5	3.9 ± 4.0 (116±5%)	1400 ± 370 (48±8%)	1.16	0.51
9b		24 ± 2	63 ± 17 (94±11%)	10000 ± 4600 (63±26%)	0.61	0.50
10a		66 ± 15	32 ± 13 (100±11%)	2900 ± 370 (65±11%)	0.29	0.49
10b		23 ± 5	4.5 ± 0.4 (59±2%)	4900 ± 1500 (56±18%)	1.29	0.36
11a		55 ± 14	22 ± 11 (108±14%)	1200 ± 95 (24±11%)	0.61	0.60
11b		22 ± 5	12 ± 1.9 (71±5%)	1400 ± 160 (65±24)%	0.31	0.65
12a		44 ± 25	33 ± 5.5 (77±11%)	8800 ± 3100 (60±21%)	0.76	0.46
12b		92 ± 39	71 ± 7.6 (124±11%)	25000 ± 10000 (61±9%)	1.07	0.33
13a	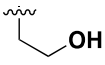	20 ± 9	16 ± 4.3 (89±7%)	6400 ± 2000 (96±14%)	0.79	0.27
13b		12 ± 1	28 ± 18 (86±12%)	3500 ± 510 (103±5)	0.24	0.51
14a		41 ± 12	35 ± 15 (91±15%)	42000 ± 12000 (78±9%)	1.37	0.44
14b		17 ± 4	8.9 ± 4.0 (69±4%)	5300 ± 2000 (47±1%)	1.17	0.49
15a		2.5 ± 1.1	2.7 ± 1.6 (103±4%)	7400 ± 4000(75±24%)	1.81	0.54
15b		21 ± 1	20 ± 5.3 (79±14%)	450 ± 140 (68±8%)	-0.36	0.35
16a		11 ± 1	49 ± 5.1 (101±10%)	24000 ± 1700 (66±16%)	1.09	0.65
16b		19 ± 8	16 ± 0.9 (95±3%)	22000 ± 1600 (161±21%)	1.15	0.62
17a		5.4 ± 0.9	7.3 ± 5.2 (96±19%)	5800 ± 220 (90±15%)	1.15	0.67
17b		61 ± 4	99 ± 33 (91±31%)	9700 ± 1000 (137±16%)	0.04	0.60
18a	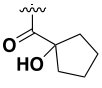	230 ± 20	58 ± 0.7 (93±2%)	6300 ± 2500 (31±1%)	0.73	0.25
18b		46 ± 6	52 ± 25 (88±7%)	4100 ± 170 (29±5%)	0.60	0.24
19a		12 ± 5	6.2 ± 3.0 (122±6%)	7100 ± 2500 (79±10%)	1.47	0.44
19b		48± 10	91 ± 12 (113±24%)	7600 ± 3000 (52±12%)	0.48	0.68

acetamide (N1 position) to be critical for optimal binding potency, as removal of one chlorine (examples **1** and **2**) or replacement of one chloro-subsitutent with a fluorine (example **3**) resulted in a loss of 4−8-fold binding affinity. The pyrrolidine substituted tetrahydro-pyran ring (C8 position) was found to be optimal for potency (example **6** and **7**) with acyclic amines displaying reduced affinity (2−5-fold). We thus focused on analogues containing the C8 pyrrolidine and N1

https://doi.org/10.1021/acschemneuro.2c00258
ACS Chem. Neurosci. 2022, 13, 1849−1856

3,4-dichlorophenylacetamide groups and looked to vary the N4 position.

To further explore the effect of substitution at the N4 position, we prepared and resolved enantiomers of the PAPPP scaffold with different R groups (Table 2) to better understand the effect of binding and functional kappa agonist activity. In addition to these, we also investigated β-arrestin coupling, the presented data for which, similarly to G-protein signaling, is normalized to the maximal signaling induced by U69,593. As indicated above for Table 1, reported values reflect a minimum of three experiments conducted on different days, with four replicates of each concentration in each experiment. Calculation of signaling bias factors used parameters of the balanced KOR agonist U69,593 as a reference compound, with positive values indicating G-protein signaling bias and negative values indicating arrestin signaling. This was conducted in accordance with our previous studies.[5,6] The PAPPP scaffold has a tendency to yield G-protein biased compounds; of a total of 28 enantiomers, 22 were found to have G-protein bias, whereas one single compound (**15b**) was found to have modest arrestin bias, in comparison to U69,593.

The pure enantiomers of compound **6** (**6a**/**6b**) showed similar profiles in both binding and functional agonism. In agreement with the affinity and efficacy data, the enantiomers **6a** and **6b** adopt an overall similar predicted binding mode (Figure 2C,E). In both enantiomers, the pyrrolidine nitrogen forms a salt bridge interaction with the Asp138$^{3.32}$ side chain and the dichlorophenyl moiety occupies a hydrophobic subpocket between TM2 and TM3. These interactions are analogously present in the docking model of U50,488 (Figure 2A). However, compared to U50,488, the PAPPP scaffold appears to have strengthened hydrogen bond interaction between the amide oxygen and the Gln115$^{2.60}$ side chain and weakened water-mediated interaction with the Tyr312$^{7.35}$ side chain (Figure 2B,D,F). Y312W mutation in KOR was previously shown to attenuate arrestin recruitment.[7] The reduced interaction with Tyr312$^{7.35}$ observed for the PAPPP scaffold is likely due to the constraint introduced by the cyclized ring constraint of piperazine, and it could provide the structural basis for its G-protein biased efficacy.

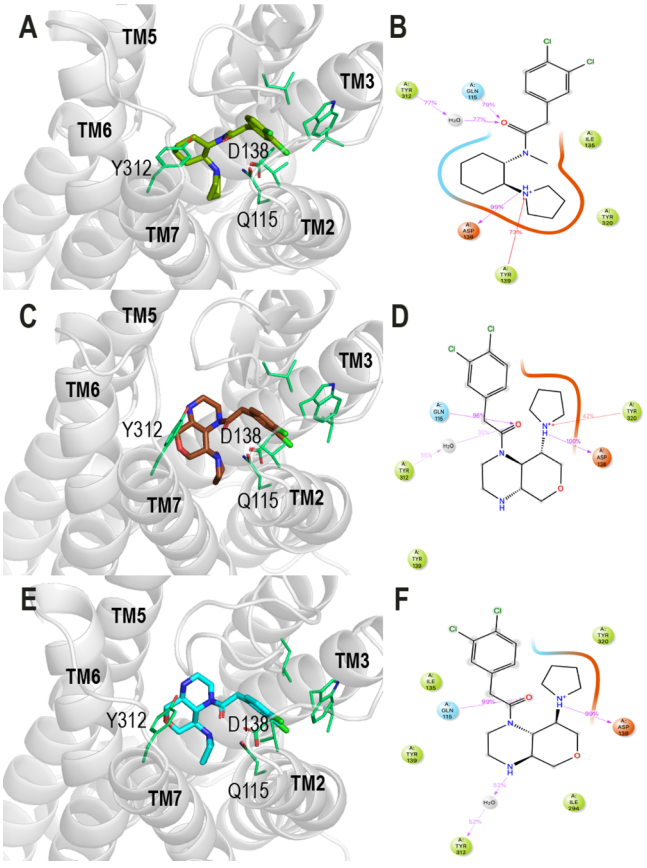

Figure 2. Docking model and receptor−ligand interaction frequency in MD simulations for U50,488 (A,B) and enantiomers **6a** (C,D) and **6b** (E,F).

Furthermore, the PAPPP series, similarly to the Wünsch series, are highly specific for KOR over MOR and DOR (MOR and DOR K_i values > 10 000 nM for compounds **6a**/**6b** and **7a**/**7b**, Supplementary Figure S1).

The R group substitution at the N4 position occupies the orthosteric binding site formed from TM3, TM5, and TM6 residues. We found that various substituents were tolerated at the N4 position (Table 2). These included sulfonamide, amide, alkyl, and even hydroxy substituted moieties. Resolved enantiomers typically displayed a similar profile in both their KOR binding potency and functional activity, but exceptions were found (examples **9a**/**9b**, **17a**/**17b**, and **19a**/**19b**). This further illustrates the modest effects that ligands can exert with respect to KOR activation, and more work will be needed to fully understand the differences seen in these enantiomeric pairs.

Interestingly, a few of the enantiomeric pairs displayed differential bias of G-proten versus β-arrestin signaling. The enantiomers of the N4 substituted analogues, **15a**/**15b**, **10a**/**10b**, and **17a**/**17b**, exhibited differential bias factor values. In these enantiomeric pairs, the enantiomer with biased efficacy also showed higher binding affinity than the other enantiomer with unbiased efficacy. The docking models of the isoxazole enantiomeric pair **15a**/**15b** with differential bias factor values indeed showed that the enantiomer with lower predicted binding affinity had re-established the interaction with Tyr312$^{7.35}$, in agreement with this interaction leading to its unbiased efficacy, whereas the dimethyl-hydroxy enantiomer pair, **14a**/**14b**, with comparable bias factor values showed reduced interaction with Tyr312$^{7.35}$ in both enantiomers (Supplementary Figure S2).

Target engagement of the PAPPP series was evaluated *in vivo* by measuring increased levels of serum prolactin, which can be used as a neuroendocrine biomarker for KOR agonist activity.[6,8,9] The observed prolactin stimulation by **7b**, the more potent in the [^{35}S]GTPγS assay of the two enantiomers of the racemic *N*-methyl analogue **7**, was blocked by pretreatment with the short acting KOR antagonist LY2444296, indicating *in vivo* KOR target engagement[10] (Figure 3). In separate experiments, stimulation of prolactin by compounds **10b** and **11b** was compared to that of the well-characterized KOR agonist, U50,488, 30 min following i.p. administration in adult male C57BL6 mice (Supplementary Figure S3).

We then investigated the serum prolactin time course of compound **7b**. Serum prolactin exhibited a rapid rise following administration of **7b** (30 mg/kg) and receded to close to control levels at the 1 h time point (Figure 4A). Similarly, in the rotarod incoordination behavioral assay, sedation measures following **7b** injection have receded to close baseline levels within 1 h (Figure 4B). These time courses reflect the PK

https://doi.org/10.1021/acschemneuro.2c00258
ACS Chem. Neurosci. 2022, 13, 1849−1856

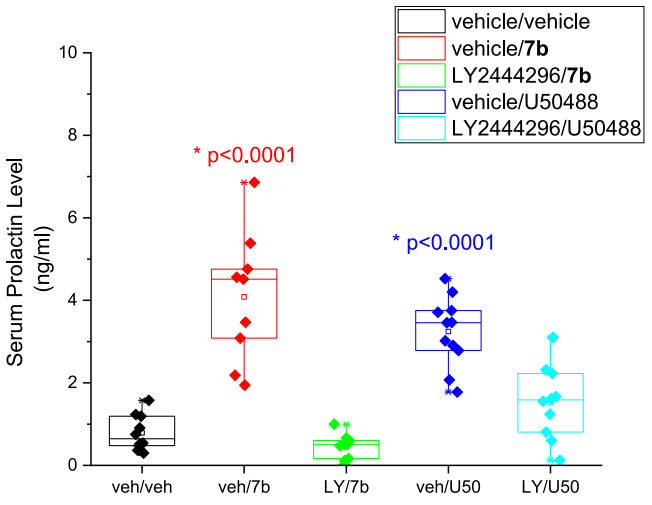

Figure 3. Prolactin stimulation by compound **7b** is mediated by KOR. Animals were injected with vehicle or 3 mg/kg LY2444296, a short-acting KOR antagonist[10,12] 15 min prior to injection of **7b** (30 mg/kg) or U50,488 (10 mg/kg), and serum prolactin levels were determined 30 min after the second injection. $N = 9-11$ for each group.*, significantly different from vehicle/vehicle group, $p < 0.0001$.

properties of the racemic compound **7** ($T_{1/2}$ = 0.69 h) (Supplementary Figure S4 and Table S1). Note that the doses for the two different assays differ, as generally KOR compounds require higher doses to cause sedative effects compared to most other KOR mediated end points.[11] This was similarly found to be the case in dose response studies of the unsubstituted PAPPP compound **6** (racemic, Supplementary Figure 5). In addition to compounds **10b**, **11b**, and **7b** (Supplementary Figures S3 and 4B, respectively), single dose (30 mg/kg, i.p.) administration of other selected compounds in the series, **6a**/**6b**, **12a**/**12b**, and **14a**/**14b**, also stimulated prolactin release 30 min following administration (see Supplementary Figure 6).

Several recent papers have investigated the effects of KOR agonists which exhibit G-protein (versus arrestin) signaling bias *in vitro* on diverse KOR mediated effects in animal models. An analogue of salvinorin A, RB-64, was shown to be substantially biased toward G-protein signaling in *in vitro* assays, relative to U69,593, in contrast to the parent compound, salvinorin A.[13] *In vivo* in mice, this compound was comparably effective as an analgesic to salvinorin A and also caused conditioned place aversion but exhibited reduced activity in producing motor incoordination and suppressing novelty-induced locomotion, suggesting a correlation of *in vitro* KOR arrestin signaling with these aspects of KOR-induced behavioral regulation. Further, RB-64 did not result in suppression of intracranial self-stimulation, which both salvinorin A and U69,593 did, indicating arrestin signaling may be involved in anhedonic effects of KOR agonists.[13]

A separately identified scaffold with KOR agonist specificity was also identified to exhibit G-protein versus arrestin signaling.[14] One of these G-protein biased KOR agonists, triazole 1.1, was further investigated in animal models,[15] with similar findings to those for RB-64. Triazole 1.1 was able to suppress itch and pain similarly to U50,488, without affecting locomotor behavior or intracranial self-stimulation, in contrast to U50,488. Importantly, systemic administration of triazole 1.1 did not result in decreased extracellular dopamine levels in microdialysis studies, in contrast with U50,488.[15]

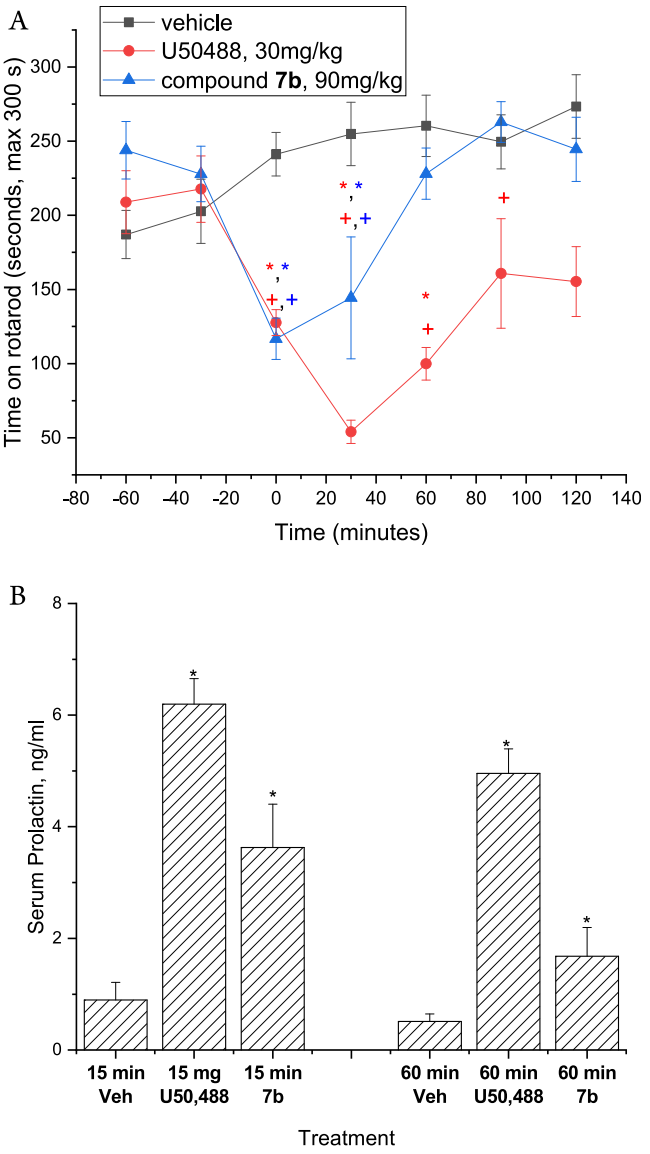

Figure 4. (A) Animals were injected with 90 mg/kg compound **7b**, vehicle, or 30 mg/kg U50,488 serving as active control ($n = 6$/group). *$p < 0.01$ versus vehicle, $^{+}p < 0.05$ versus baseline measures. (B) Animals were injected with 30 mg/kg compound **7b**, with 10 mg/kg U50,488 serving as a control. 7−8 animals were included in each dosing group. *$p < 0.05$ versus vehicle.

Similarly we found that the extent of KOR-mediated G-protein versus arrestin signaling bias in a series of trialkylamine derivatives was inversely correlated with sedative effects as measured with increased incoordination in the rotarod assay.[6] This inverse correlation of G-protein bias with rotarod sedation was found to hold across multiple structural classes of KOR agonists.[5] However, one recent paper suggests that *in vivo* incoordination is not in fact correlated with *in vitro* KOR arrestin signaling, comparing the effects of a nalfurafine analogue, 42B, with nalfurafine.[16] Although the structural modification was modest, involving the removal of the hydroxyl substituent at position 3 of the morphinan backbone, *in vitro* and *in vivo* potency was highly reduced. Nalfurafine and 42B both exhibited modest G protein bias, but 42B demonstrated greater rotarod incoordination and locomotor inhibition at doses which were effective in analgesic and antipruritic models. This may reflect the extraordinary *in vivo*

https://doi.org/10.1021/acschemneuro.2c00258
ACS Chem. Neurosci. 2022, 13, 1849−1856

potency of nalfurafine, which at higher doses results in substantial rotarod incoordination.[11] An additional recent study of salvinorin A analogues found the G-protein biased 16-bromo substituted salvinorin A to produce incoordination comparable to that of the balanced analogue 16-ethinyl substituted salvinorin A[17] while not yielding anxiogenic effects in an elevated zero maze. The reasons for this discrepancy of *in vivo* effects of this G-protein biased compound with previously reported studies was noted, but it cannot yet be fully explained.

The series of largely G-protein biased (versus β_2-arrestin, in comparison to U69,593) compounds, exhibiting centrally mediated *in vivo* KOR activity, we have discussed here will be valuable tools in assessing the prospects of biased KOR agonists as potential therapeutic agents. The mechanism of KOR mediated prolactin release is not worked out and is beyond the scope of the current studies. Our earlier studies suggest that the stimulation of prolactin release is *not* arrestin mediated,[5,6] which is suggestive but not definitive of a G-protein mediated mechanism. In particular, enantiomeric pairs which show substantial differences in *in vitro* bias factors, such as **10a**/**10b** and **15a**/**15b**, may help delineate the effects of KOR bias on overall behavioral profile and therapeutic potential in ongoing studies in rodent models of substance use disorders and future studies in models of analgesia and pruritus.

METHODS

Cell Culture. U2OS cells expressing a human kappa opioid receptor construct were obtained from DiscoverX (PathHunter U2OS OPRK1 β-arrestin-2 cell line, DiscoverX, Fremont, CA, USA). These cells are grown in 37 °C/5%CO_2 in Eagle's Minimum Essential Medium. Cells were prepared for assays as described below. Additional cell lines, also obtained from DiscoverX, include CHO-K1 cells expressing a human mu opioid receptor construct (PathHunter CHO-K1 OPRM1 β-arrestin-2 cell line) or a human delta opioid receptor construct (PathHunter CHO-K1 OPRD1 β-arrestin-2 cell line), grown similarly in F-12K medium.

Compound Information. U50,488 and U69,593 were obtained from Sigma-Aldrich. LY2444296 was synthesized by WuXi Apptech (CRO, Shanghai, China), following initiation of studies with a portion of this compound gifted by Eli Lilly and Co. [^{3}H]U69,593, [^{3}H][D-Ala^2, *N*-MePhe^4, Gly-ol]-enkephalin ([^{3}H]DAMGO) [^{3}H][D-Pen^{2,5}]-enkephalin ([^{3}H]DPDPE) for binding assays for KOP-r, MOP-r, and DOP-r, and [^{35}S]GTPγS were obtained from PerkinElmer. The compounds were reconstituted at a concentration of 20 mM in dimethylsulfoxide (Sigma-Aldrich) for use in biological assays.

Radioligand Binding Assays. Membranes were prepared from cell lines for radioligand binding assays using [^{3}H]U69,593 for KOP-r, [^{3}H][D-Ala$_2$, *N*-MePhe4, Gly-ol]-enkephalin ([^{3}H]DAMGO) for MOP-r, and [^{3}H][D-Pen2,5]-enkephalin ([^{3}H]DPDPE) for DOP-r. Cells were scraped and homogenized in membrane buffer (10 mM Tris, 100 mM NaCl, 1 mM EDTA, pH 7.4) with a tissue tearor homogenizer, followed by centrifugation (20 000*g*, 30 min, 4 °C), and membrane pellets were stored at −80 °C until the day of assay. For the binding curves and determination of K_i of each compound, 20 mM DMSO stocks were diluted 1000-fold to 20 μM, with subsequent 4-fold dilution for each concentration, for a total of 11 concentrations (with the lowest concentration for each compound being 76.2 pM). Assay buffer (50 mM Tris, 100 mM NaCl, pH 7.4) was used to resuspend membrane pellets, followed by dounce homogenization. Membranes were first treated with the appropriate concentration of test compound, followed by shaking, and then incubated with 1 nM [^{3}H]U69,593, 1 nM [^{3}H]DAMGO, or 1 nM [^{3}H]DPDPE for 60 min at 30 °C, in a total volume of 220 μL. Nonspecific binding was assessed using 10 μM norbinaltorphimine (KOP-r), 10 μM naltrexone (MOP-r), or 10 μM naltrindole (DOP-r). Membranes with bound ligand were collected on Whatman GF/B filter paper (Brandel) through a harvester. Bound ligand was quantified using a TriCarb-2900TR scintillation counter (Packard) following addition of 4.5 mL of ReadySafe scintillation fluid (Beckman Coulter). All samples were run in quadruplicate.

[^{35}S]GTPγS Assay. Similar to binding assays, membranes were prepared from U20S-hOPRK1 cells, scraped from tissue culture plates, homogenized in membrane buffer, centrifuged, and stored at −80 °C. Membranes (10 μg) were coincubated with 0.1 nM [^{35}S]GTPγS and respective concentrations of test compounds at 30 °C for 20 min, in a total volume of 220 μL. As described with the binding assays, membranes with bound [^{35}S]GTPγS were collected on filter paper through a harvester and bound [^{35}S]GTPγS was quantified using a TriCarb-2900TR scintillation counter (Packard) following addition of 4.5 mL of scintillation fluid. All samples were run in quadruplicate.

β-Arrestin-2 Assay. Assay was conducted using the PathHunter Detection Kit obtained from DiscoverX. Cells stably expressing human kappa opioid receptors (PathHunter U2OS hOPRK1 with a C-terminal fusion protein coexpressed with a complementary β-arrestin-2 fusion) were plated on 384-well plates. For the assay, the cells in each well were coincubated with various concentrations of test compound for 90 min at 37 °C. This was followed by the addition of a pro-chemiluminescent substrate of β-galactosidase enzyme and incubation for another 60 min at 37 °C, yielding a chemiluminescence product. Chemiluminescence was measured using a Synergy Neo microplate reader (BioTek). All samples were run in quadruplicate.

Calculation of Bias Factor. Bias factors were calculated utilizing a modified competitive model analysis method,[1,2] as previously described.[3,4] Briefly, LogRA is a measure incorporating a comparison of the affinity and efficacy of test ligands with that of a reference compound (U69,593) in stimulating KOPr signaling. Comparison of log RA in the [^{35} S]GTPγS stimulation assay with the log RA determined in the β-arrestin-2 assay allows determination of relative bias in one assay versus the other compared to the reference compound U69,593.

Molecular Modeling and Simulation. The binding mode of U50,488 and PAPPP series compounds was predicted by docking and simulation based on the crystal structure of the active-state human KOP (PDB: 6B73) using Schrödinger's Glide docking program and Desmond molecular dynamics simulation package (Schrodinger release 2020-4). The receptor protein structure was prepared using the Protein Preparation Wizard in Maestro with default settings, filling in the missing loop residues in ECL2, ECL3, and ICL3 with Prime and restoring the WT residue Ile135(3.29). The ligand structures were prepared using LigPrep in Maestro with default settings and parametrized for the OPLS3e force field using Force Field Builder. The receptor−ligand complex was embedded in the POPC lipid bilayer using the OPM alignment, and with a 16 Å buffer size box and 0.15 M salt concentration. The molecular dynamics simulation of the receptor−ligand complex in the lipid environment was performed in NPT ensemble at 300 K for 30−90 ns until the ligand and protein RMSDs converged. The receptor−ligand interaction frequencies were obtained from the last 15 ns segment of simulation trajectory for each complex. Since the nanobody was removed, a weak constraint (force constant k = 1) was placed during the simulation on the TM5 and TM6 intracellular segments (residues Pro238(5.50) to Pro289(6.50)) to maintain the active-state conformation of the receptor. The MMGBSA ligand binding free energy was calculated using Prime in Maestro.

Animals for *In Vivo* Assay. All *in vivo* experiments were performed with adult (9−15 week) male C57BL6 mice. Animals were housed 4/cage in dedicated stress-minimized cabinets under 12 h on/12 h off, 7AM to 7PM. Following receipt, animals were allowed 1 week for acclimation, prior to beginning of daily handling, rotarod training, and mock injections. All studies were approved by the Institutional Animal Care and Use Committee of Rockefeller University.

Formulation of Compounds for *In Vivo* Assays. For *in vivo* studies, the compounds were dissolved in 10% ethanol, 10% Tween-

https://doi.org/10.1021/acschemneuro.2c00258
ACS Chem. Neurosci. 2022, 13, 1849−1856

80, 80% distilled deionized water, at the specified dose administered intraperitoneally (i.p.) in a total volume of 5 μL/g for each animal.

Rotarod. A rotarod apparatus capable of testing five animals at the same time was used (IITC Life Science, Woodland Hills, CA, USA). For training on the apparatus prior to the experiment, animals were given exposure to the stationary apparatus for 1−2 min, 1−2 days prior to initial placement on rotarod apparatus. The rod rotated initially at 3 rpm, and this rate was linearly increased to 30 rpm over the course of 300 s (5 min). Upon each animal falling from the rod, its time was recorded individually. The maximum time for each animal trial was 300 s (if the animal did not fall). Animals were subject to at minimum 3 days of training, after an acclimation session on stationary rods. On the day of the experiment, two successive baseline sessions, separated by 30 min, were used to determine average time until animals fall. Animals were then injected i.p. with vehicle, experimental compound, or U50,488 (10 mg/kg) as a control KOR agonist and immediately tested on the rotarod apparatus (test begun 0−2 min after injection), followed by tests at 30 and 60 min following injections, unless otherwise indicated.

Prolactin. Generally, the same cohort of animals used to assess rotarod was then used to assess prolactin releasing effects of the experimental compounds, in a separate experiment conducted at least 1 week later. Following mock injection habituation, animals were injected i.p. with vehicle, experimental compound, or U50,488 (10 mg/kg) 30 min prior to blood collection, followed by serum preparation. When applicable, mice were also injected i.p. with KOPr antagonist LY2444296 or vehicle 15 min prior to treatment, to verify that the effects are mediated by KOPr. Animals were subject to rapid decapitation and collection of trunk blood in serum collection tubes 30 min after injection (except where otherwise noted). Serum was prepared within 2 h and then diluted 5-fold in assay buffer for determination of serum prolactin levels using a commercially available enzyme-linked immunoassay specific for mouse prolactin (AbCam, Cambridge, UK).

Statistics for Animal Experiments. Statistica 13.0 software (TIBCO Software, Palo Alto, CA) was used to analyze rotarod and prolactin experiments. In the case of rotarod experiments, two-way ANOVA with repeated measures (condition/dose × time, with repeated measures on time) was used to analyze each experiment and determine effects and interactions of condition/dose and time. For prolactin experiments, one-way ANOVA was used to examine the effects of condition or dose. Newman−Keuls posthoc tests were utilized to evaluate significant differences within each experiment.

■ ASSOCIATED CONTENT

Supporting Information

The Supporting Information is available free of charge at https://pubs.acs.org/doi/10.1021/acschemneuro.2c00258.

Compound preparation and characterization, mouse pharmacokinetic study, dose response of rotarod sedation and prolactin stimulation, and molecular docking of compounds **16a,b** and **17a,b** (PDF)

■ AUTHOR INFORMATION

Corresponding Author

Brian Reed − *Laboratory of the Biology of Addictive Diseases, The Rockefeller University, New York, New York 10065, United States;* orcid.org/0000-0002-5211-366X; Phone: +1-212-327-8234; Email: reedb@rockefeller.edu; Fax: +1-212-327-8574

Authors

Michael Miller − *Tri-Institutional Therapeutics Discovery Institute, New York, New York 10021, United States*

Mayako Michino − *Tri-Institutional Therapeutics Discovery Institute, New York, New York 10021, United States*

Eduardo R. Butelman − *Laboratory of the Biology of Addictive Diseases, The Rockefeller University, New York, New York 10065, United States*

Ariel Ben-Ezra − *Laboratory of the Biology of Addictive Diseases, The Rockefeller University, New York, New York 10065, United States;* Present Address: SUNY Downstate Health Sciences University College of Medicine, Brooklyn, New York, 1120, United States

Philip Pikus − *Laboratory of the Biology of Addictive Diseases, The Rockefeller University, New York, New York 10065, United States;* Present Address: Georgetown University School of Medicine, Washington, DC, 20007, United States

Michelle Morochnik − *Laboratory of the Biology of Addictive Diseases, The Rockefeller University, New York, New York 10065, United States*

Yuli Kim − *Laboratory of the Biology of Addictive Diseases, The Rockefeller University, New York, New York 10065, United States*

Amy Ripka − *Lucy Therapeutics, Cambridge, Massachusetts 02139, United States*

Joseph Vacca − *J. Vacca Consulting LLC, Telford, Pennsylvania 18969, United States*

‡**Mary Jeanne Kreek** − *Laboratory of the Biology of Addictive Diseases, The Rockefeller University, New York, New York 10065, United States*

Complete contact information is available at: https://pubs.acs.org/10.1021/acschemneuro.2c00258

Author Contributions

†These authors contributed equally. B.R., E.B., and M.J.K. designed the overall project. Mi.Mil., A.R., and J.V. designed the compounds and directed the synthetic pathways. Ma. Mic. conducted molecular modeling studies and interpretations. B.R. and M.J.K. designed *in vivo* experiments and interpreted results. A.B.E, P.P., Y.K., and Mic.Mor. performed binding, signaling, and *in vivo* experiments. B.R. conducted data analysis.

Funding

Funding was provided by the Dr. Miriam and Sheldon Adelson Research Foundation and the Robertson Therapeutic Development Fund. The authors gratefully acknowledge the support to the project generously provided by the Tri-Institutional Therapeutics Discovery Institute (TDI), a 501(c) (3) organization. TDI receives financial support from Takeda Pharmaceutical Company, TDI's parent institutes (Memorial Sloan Kettering Cancer Center, The Rockefeller University and Weill Cornell Medicine) and from a generous contribution from Mr. Lewis Sanders and other philanthropic sources.

Notes

The authors declare no competing financial interest.

‡Deceased March 27, 2021.

This article is a posthumous publication for our admired but recently departed coauthor, Mary Jeanne Kreek.

■ ACKNOWLEDGMENTS

The authors would like to acknowledge technical contributions from several individuals, including Joshua Hillman, Dr. Amelia Dunn, Alexandra Dunn, Catherine Guariglia, and Jose Erazo. Further we gratefully acknowledge Drs. Bruce Conway, Stacia Kargman, Nigel Liverton, Peter Meinke, and Leigh Baxt for intellectual input. We are grateful to Dr. Linda Rorick-Kehn for

facilitating the generous provision by Eli Lilly and Co. of the KOR antagonist LY2444296. We also acknowledge the Rockefeller University High-Throughput and Spectroscopy Resource Center and the Comparative Bioscience Center for instrumentation and animal housing and care.

■ ABBREVIATIONS

DOP-r, delta opioid receptor; GPCR, G-protein coupled receptor; GTPγS, guanosine 5′-*O*-[gamma-thio]triphosphate; K_i, Inhibition constant; KOP-r, kappa opioid receptor; MOP-r, mu opioid receptor; PAPPP, dichlorophenylacetamide-pyrrolidinyl-pyranopiperazine; CI, confidence interval

■ REFERENCES

(1) Miller, M.; Reed, B. Recent progress in kappa and mu opioid receptor targeted ligands. In *2020 Medicinal Chemistry Reviews*; Bronson, J. J., Ed.; American Chemical Society Division of Medicinal Chemistry, 2020; Vol. *55*, pp 102−116.
(2) Violin, J. D.; Lefkowitz, R. J. β-Arrestin-biased ligands at seven-transmembrane receptors. *Trends Pharmacol. Sci.* **2007**, *28*, 416−422.
(3) Bourgeois, C.; Werfel, E.; Schepmann, D.; Wünsch, B. Combination of cyclohexane and piperazine based κ-opioid receptor agonists: Synthesis and pharmacological evaluation of trans,trans-configured perhydroquinoxalines. *Bioorg. Med. Chem.* **2014**, *22*, 3316−3324.
(4) Bourgeois, C.; Werfel, E.; Galla, F.; Lehmkuhl, K.; Torres-Gómez, H.; Schepmann, D.; Kögel, B.; Christoph, T.; Straßburger, W.; Englberger, W.; Soeberdt, M.; Hüwel, S.; Galla, H.-J.; Wünsch, B. Synthesis and Pharmacological Evaluation of 5-Pyrrolidinylquinoxalines as a Novel Class of Peripherally Restricted κ-Opioid Receptor Agonists. *J. Med. Chem.* **2014**, *57*, 6845−6860.
(5) Dunn, A. D.; Reed, B.; Erazo, J.; Ben-Ezra, A.; Kreek, M. J. Signaling Properties of Structurally Diverse Kappa Opioid Receptor Ligands: Toward in Vitro Models of in Vivo Responses. *ACS Chem. Neurosci.* **2019**, *10*, 3590−3600.
(6) Dunn, A. D.; Reed, B.; Guariglia, C.; Dunn, A. M.; Hillman, J. M.; Kreek, M. J. Structurally Related Kappa Opioid Receptor Agonists with Substantial Differential Signaling Bias: Neuroendocrine and Behavioral Effects in C57BL6Mice. *international journal of neuropsychopharmacology* **2018**, *21*, 847−857.
(7) Che, T.; Majumdar, S.; Zaidi, S. A.; Ondachi, P.; McCorvy, J. D.; Wang, S.; Mosier, P. D.; Uprety, R.; Vardy, E.; Krumm, B. E.; Han, G. W.; Lee, M. Y.; Pardon, E.; Steyaert, J.; Huang, X. P.; Strachan, R. T.; Tribo, A. R.; Pasternak, G. W.; Carroll, F. I.; Stevens, R. C.; Cherezov, V.; Katritch, V.; Wacker, D.; Roth, B. L. Structure of the Nanobody-Stabilized Active State of the Kappa Opioid Receptor. *Cell* **2018**, *172*, 55−67.e15.
(8) Butelman, E. R.; Ball, J. W.; Kreek, M. J. Comparison of the discriminative and neuroendocrine effects of centrally penetrating kappa-opioid agonists in rhesus monkeys. *Psychopharmacology (Berl)* **2002**, *164*, 115−120.
(9) Chang, C.; Byon, W.; Lu, Y.; Jacobsen, L. K.; Badura, L. L.; Sawant-Basak, A.; Miller, E.; Liu, J.; Grimwood, S.; Wang, E. Q.; Maurer, T. S. Quantitative PK-PD model-based translational pharmacology of a novel kappa opioid receptor antagonist between rats and humans. *Aaps j* **2011**, *13*, 565−575.
(10) Valenza, M.; Butelman, E. R.; Kreek, M. J. Effects of the novel relatively short-acting kappa opioid receptor antagonist LY2444296 in behaviors observed after chronic extended-access cocaine self-administration in rats. *Psychopharmacology* **2017**, *234*, 2219−2231.
(11) Dunn, A.; Windisch, K.; Ben-Ezra, A.; Pikus, P.; Morochnik, M.; Erazo, J.; Reed, B.; Kreek, M. J. Modulation of cocaine-related behaviors by low doses of the potent KOR agonist nalfurafine in male C57BL6 mice. *Psychopharmacology (Berl)* **2020**, *237*, 2405−2418.
(12) Butelman, E. R.; McElroy, B. D.; Prisinzano, T. E.; Kreek, M. J. Impact of Pharmacological Manipulation of the κ-Opioid Receptor System on Self-grooming and Anhedonic-like Behaviors in Male Mice. *J. Pharmacol Exp Ther* **2019**, *370*, 1−8.
(13) White, K. L.; Robinson, J. E.; Zhu, H.; DiBerto, J. F.; Polepally, P. R.; Zjawiony, J. K.; Nichols, D. E.; Malanga, C. J.; Roth, B. L. The G protein-biased κ-opioid receptor agonist RB-64 is analgesic with a unique spectrum of activities in vivo. *J. Pharmacol Exp Ther* **2015**, *352*, 98−109.
(14) Zhou, L.; Lovell, K. M.; Frankowski, K. J.; Slauson, S. R.; Phillips, A. M.; Streicher, J. M.; Stahl, E.; Schmid, C. L.; Hodder, P.; Madoux, F.; Cameron, M. D.; Prisinzano, T. E.; Aubé, J.; Bohn, L. M. Development of functionally selective, small molecule agonists at kappa opioid receptors. *J. Biol. Chem.* **2013**, *288*, 36703−36716.
(15) Brust, T. F.; Morgenweck, J.; Kim, S. A.; Rose, J. H.; Locke, J. L.; Schmid, C. L.; Zhou, L.; Stahl, E. L.; Cameron, M. D.; Scarry, S. M.; Aubé, J.; Jones, S. R.; Martin, T. J.; Bohn, L. M. Biased agonists of the kappa opioid receptor suppress pain and itch without causing sedation or dysphoria. *Sci. Signal.* **2016**, *9*, ra117.
(16) Cao, D.; Huang, P.; Chiu, Y. T.; Chen, C.; Wang, H.; Li, M.; Zheng, Y.; Ehlert, F. J.; Zhang, Y.; Liu-Chen, L. Y. Comparison of Pharmacological Properties between the Kappa Opioid Receptor Agonist Nalfurafine and 42B, Its 3-Dehydroxy Analogue: Disconnect between in Vitro Agonist Bias and in Vivo Pharmacological Effects. *ACS Chem. Neurosci.* **2020**, *11*, 3036.
(17) Paton, K. F.; Biggerstaff, A.; Kaska, S.; Crowley, R. S.; La Flamme, A. C.; Prisinzano, T. E.; Kivell, B. M. Evaluation of Biased and Balanced Salvinorin A Analogs in Preclinical Models of Pain. *Front. Neurosci.* **2020**, *14*, 765.

https://doi.org/10.1021/acschemneuro.2c00258
ACS Chem. Neurosci. 2022, 13, 1849−1856